Molecular Crystals and Liquid Crystals
Publication details, including instructions for authors and subscription information:
http://www.informaworld.com/smpp/title~content=t713644168

Optical Diffraction Effects of Grating Cells Fabricated Using Polymer-Dispersed Liquid Crystals

J. -W. Han[a]
[a] Department of Physics, Daegu University, Gyungsan, Republic of Korea

First published on: 18 January 2011

To cite this Article Han, J. -W.(2011) 'Optical Diffraction Effects of Grating Cells Fabricated Using Polymer-Dispersed Liquid Crystals', Molecular Crystals and Liquid Crystals, 534: 1, 69 — 80
To link to this Article: DOI: 10.1080/15421406.2011.536483
URL: http://dx.doi.org/10.1080/15421406.2011.536483

Mol. Cryst. Liq. Cryst., Vol. 534: pp. 69–80, 2011

ISSN: 1542-1406 print/1563-5287 online
DOI: 10.1080/15421406.2011.536483

Taylor & Francis
Taylor & Francis Group

Optical Diffraction Effects of Grating Cells Fabricated Using Polymer-Dispersed Liquid Crystals

J.-W. HAN

Department of Physics, Daegu University, Gyungsan, Republic of Korea

In this work, we investigated the optical properties of diffraction gratings fabricated using in-plane switching cells and polymer-dispersed liquid crystal (LC) materials. The diffraction intensities of the zeroth and first diffraction orders strongly depend on the applied voltage as well as the polarization of light. In particular, a study of the intensity of the first diffraction order for the p-polarized light as a function of the applied voltage shows a bell-shaped peak; the peak voltage can be controlled by varying the preparation process and LC concentrations. Our results demonstrate that these cells are promising for developing switchable diffraction gratings.

Keywords Diffraction; grating; IPS; Kelvin force; PDLC

Introduction

Liquid crystal (LC) gratings have been intensively investigated for potential application in optical communication and switchable optical diffraction devices [1–5]. There are a variety of ways to construct grating structures using LC materials [6–10]. One method of fabricating optical diffraction gratings is to construct a periodic phase-shift pattern in the LC layer. These gratings can be classified into three groups according to the method of building the periodic phase-shift pattern.

In the first group, the LC is sandwiched between two glass plates with appropriately patterned electrodes on each surface. One plate usually has a periodic striped structure of indium tin oxide (ITO) electrodes and the other has either a uniform ITO electrode or no electrodes. The plate surfaces are treated to induce an alignment of LC molecules in a preferred direction. When a voltage is applied between two plates, a periodically changing electric field is produced across the plates. In a region where the electric field is strong, LC molecules are aligned along the local electric field, whereas in a region where the electric field is weak, the alignment of LC molecules remains unchanged. When light is incident on this cell, a periodic phase shift of incident light is produced.

In the second group, a homogeneous mixture of a liquid crystal and a monomer material containing an appropriate amount of photo-initiator is sandwiched between two glass plates, one of which has patterned ITO electrodes. When ultraviolet (UV)

Address correspondence to J.-W. Han, Department of Physics, Daegu University, Gyungsan 712-714, Republic of Korea. E-mail: hanwoo@daegu.ac.kr

light is irradiated on this cell, the mixture is polymerized, causing the liquid crystal to separate from the polymer matrix and to form LC droplets. This resulting material is called a polymer-dispersed liquid crystal (PDLC). Applying a voltage to the patterned ITO electrodes generates a correspondingly patterned electric field across the plates. If a saturating voltage is applied between the patterned electrodes during the UV curing process, the patterned alignments of LC molecules generated by the patterned electric field can be permanently fixed. However, in this case, because the director of LC molecules inside droplets can still be controlled by the electric field, the cell can be used as a switchable grating. Other processes commonly employed to produce gratings are holographic PDLC (H-PDLC) and the photo-mask techniques [11–13].

In the third group, the surface treatment of plates is used to produce a patterned LC alignment. In this case, LC molecules are aligned according to the patterned structure of the alignment layer. Patterning LC alignment by controlling the surface properties is a promising technique. Common ways of producing patterned surface treatments are multiple rubbings combined with a photolithography process [14] and photo-induced alignment using a linearly polarized UV laser [15,16].

In this work, we studied the optical properties of switchable gratings constructed with PDLC materials and in-plane-switching (IPS) cells. The experimental results demonstrate that these cells function well as optical gratings by generating a periodic phase modulation of incoming light.

Experimental

In this work, we prepared gratings using empty IPS cells purchased from Instec (Boulder, CO, USA). The schematic drawing of an IPS cell is shown in Fig. 1a. The lower glass plate has patterned ITO electrodes on the inner surface, and the upper one has no electrodes. The width and inter-electrode spacing of the electrodes are 18 and 11 μm, respectively, and the pitch of the electrodes is 29 μm. The cell gap between the two plates was set by 9-μm glass spacers. Both glass substrates were coated with a polyimide (PI) layer and rubbed along the long direction of the electrodes to induce homogeneous alignment perpendicular to the electric field.

When a saturating voltage is applied between the electrodes in an IPS cell, an inhomogeneous electric field is generated in the cell gap region. In this case, LC molecules and monomer material experience an inhomogeneous electric field and move to a higher electric field due to the Kelvin polarization force [17]. When a dielectric material is in an inhomogeneous electric field, the Kelvin force is given by

$$\vec{F} = (\vec{P} \cdot \nabla)\vec{E}, \tag{1}$$

where $\vec{P}$ is the polarization of the dielectric material and $\vec{E}$ is the electric field. When LC droplets are homogeneously dispersed in a monomer matrix, the net Kelvin force on the LC droplets is calculated as

$$\vec{F}_{net} = \frac{1}{2}(\varepsilon_{LC} - \varepsilon_m)\nabla(E^2). \tag{2}$$

ε_{LC} and ε_m are the dielectric constants of the LC droplets and the monomer material, respectively. Because a small amount of LC remains dissolved in the monomer

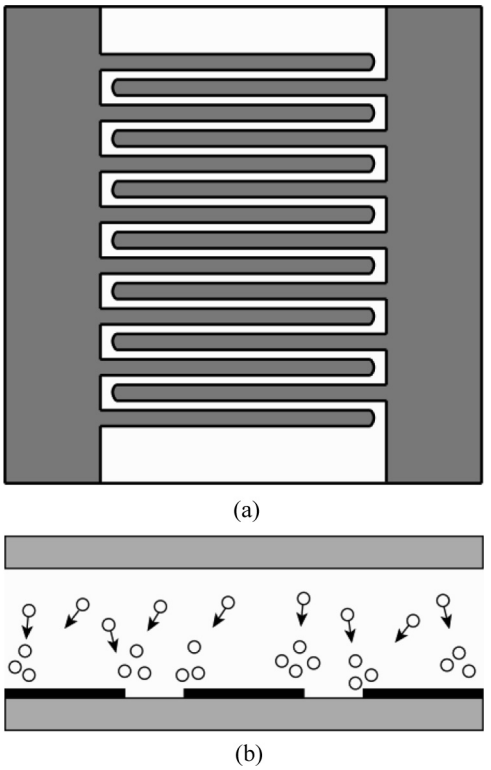

Figure 1. Schematic drawings of (a) in-plane switching electrodes on the lower glass plate and (b) enforced movement of LC droplets in the direction of a higher electric field.

matrix, the actual dielectric constant of the monomer material is a little different from that of the pure monomer material. Because $\varepsilon_{LC} \approx \varepsilon_{\|}$ and ε_{LC} is larger than ε_m in our case, the net driving force on LC droplets is exerted in the direction of the higher electric field. This process is illustrated in Fig. 1b.

We prepared grating cells with a commercially available liquid crystal mixture (E7, $\varepsilon_{\|} = 19.0$, $\Delta\varepsilon = +13.8$, $n_o = 1.5216$, $\Delta n = +0.2246$) and a monomer material (NOA65, $n = 1.524$). The liquid crystal, E7, is a eutectic mixture of nematic liquid crystals obtained from Merck Industrial Chemicals (Damstadt, Germany). The monomer material, NOA65, was purchased from Norland Products, Inc (Cranbury, NJ, USA. These materials were used as received. E7 has a nematic-isotropic (N-I) transition at 61°C. NOA65 can be cured using ultraviolet light with a maximum absorption within the range 350–380 nm. According to the manufacturer's data sheets, fully cured NOA65 has a refractive index of 1.524 and a dielectric constant of ~4.0 at 1 MHz.

Homogeneous mixtures of E7 and NOA65 were introduced into the gap between two glass plates using capillary filling at 65°C and then the cells were slowly cooled to 30°C to induce phase separation of the LC droplets from the monomer material. We observed the cells in situ with an optical microscope to control the experimental parameters. At this stage, we used two distinct processes to manufacture two groups of grating cells. For one group of cells (A group), we first applied a saturating voltage of 135 V_{rms} between striped electrodes to induce LC–monomer separation by the

Kelvin polarization force and then irradiated it with ultraviolet (UV) light to fix the separation permanently. The other group of cells (B group) was prepared in the same way except that no voltage was applied between the electrodes during UV irradiation. UV irradiation for the polymerization process was made from a spotlight source (Model L9588-1, Hamamatsu) at 20°C. The driving signal of the applied voltage was sinusoidal at 1 kHz, and the applied voltage was the root mean square (rms) voltage, unless otherwise specified. The electro-optical properties of the cells were measured with an He-Ne laser (5 mW, 632.8 nm) and a power meter (Model PM100, Thorlabs). The PDLC morphology was studied with an optical microscope equipped with a charge coupled device (CCD) camera (Model CH40, Olympus). The cell temperature for microscopic studies and polymerization was controlled using an Instec hot stage (model BS60 with an optional 95°C limit).

Results and Discussion

In the present work, we fabricated two groups of grating cells (groups A, B) while varying the E7 content (53, 75 wt%). The sample characteristics are summarized in Table 1. The optical microscope photographs of a 53 wt% cell (cell 53A) before and after UV curing are shown in Figs. 2a and 2b, and that of a 75 wt% cell (cell 75A) is shown in Fig. 2c for comparison. Note that Fig. 2a was obtained before UV curing and with 135 V_{rms} applied, whereas Fig. 2b was taken after UV curing and with no voltage applied. It is clearly seen in Fig. 2a that the LC builds up around the edges of each electrode stripe. Because of polymerization, this accumulated LC remains in the region even after removal of the electric field, as seen in Fig. 2b.

This phenomenon can be explained by the Kelvin force. Because the gradient in the squared magnitude of the electric field is the steepest near the edges of an electrode stripe and is relatively flat in the inter-electrode region and the center region of an electrode, the Kelvin force drives the LC to move toward the region near the edges of electrode stripes and monomer material to move away from the edge region of the electrode to the center region of the electrode and the inter-electrode region. We obtained similar experimental results for cell 75A as presented in Fig. 2c, which were obtained after removing the electric field.

Cell 53B

We measured the dependences of the diffracted intensities on the voltage for cell 53B, as shown in Figs. 3a and 3b. For these measurements, we used two linearly polarized

Table 1. Sample characteristics

Sample	Preparation process	LC concentration (wt%)
Cell 53A	A	53
Cell 53B	B	53
Cell 75A	A	75

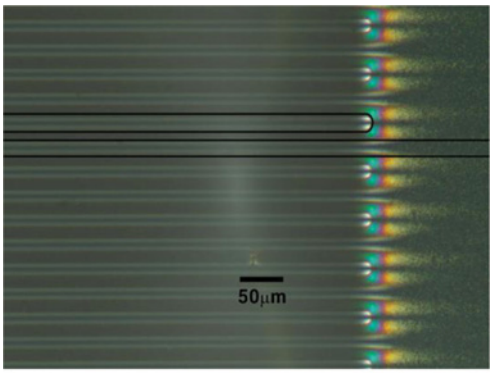

(a)

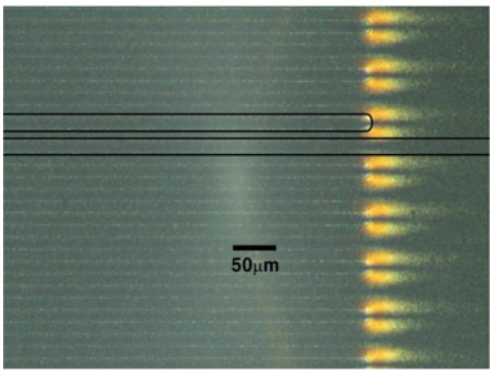

(b)

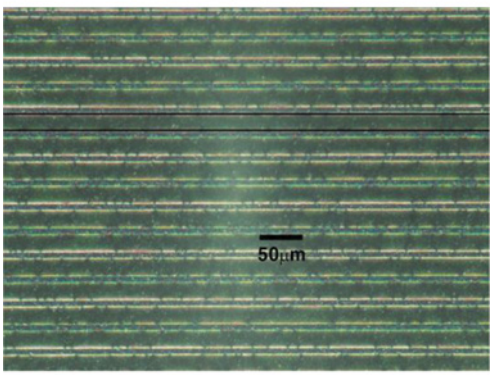

(c)

Figure 2. Optical micrographs of (a) cell 53A before UV curing, (b) cell 53A after UV curing, and (c) cell 75A after UV curing. The horizontal electrodes are marked. The images were obtained between crossed polarizers at room temperature.

lights whose planes of polarization were perpendicular to each other. These lights were incident normal to the grating cells. In our case, one light was polarized in the direction parallel to the electrode stripes and the other was at a right angle to them. These lights are referred to as the *s*- and *p-polarized lights*, respectively.

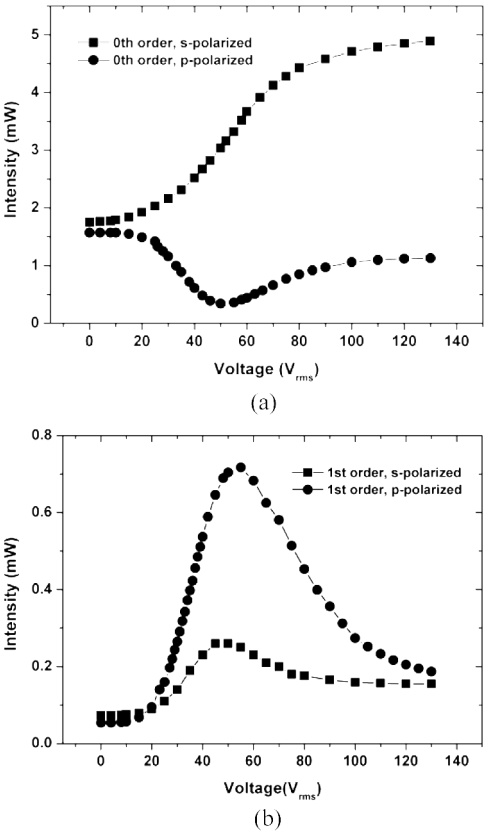

Figure 3. Diffracted intensities of cell 53B for the s- and p-polarized lights: (a) the zeroth diffraction order and (b) the first diffraction order.

Figure 3a shows the intensities of the zeroth diffraction order for the s- and p-polarized lights as a function of the applied voltage. The diffracted intensity for the s-polarized light increases monotonically with increasing voltage, whereas that for the p-polarized light first decreases, reaching a minimum at ~50 V; afterwards, it increases, eventually approaching a constant value. Figure 3b shows the intensities of the first diffraction order for the s- and p-polarized lights as a function of the applied voltage. Interestingly, the intensities of both s- and p-polarized lights initially increase with increasing voltage, reach maxima in the range of 50–55 V, and then decrease, eventually approaching a common value. Here, we define the voltage at which the intensity curve reaches a maximum as the peak voltage, V_p.

For cell 53B, LC droplets are uniformly dispersed in the polymer matrix and their director orientations are randomly distributed. In this case, the intensities at 0 V for the s- and p-polarized lights should be indistinguishable from each other due to the optical isotropy of the material. This was actually observed for the zeroth and first diffraction orders in Figs. 3a and 3b. Because of the optical isotropy, this cell also shows no diffraction effects at 0 V. As the voltage increases, the directors of LC droplets tend to align in the direction of the electric field. Upon application of a voltage, the electric field is the strongest in the edge regions of the electrodes,

the weakest in the center regions of electrodes, and intermediate in the inter-electrode regions. It also decreases by moving from the lower to the upper plate. Accordingly, with increasing voltage, the degree of LC alignment in the cell space becomes different from region to region. As a result, the cell begins to generate grating effects for incoming light, but specific optical effects are quite different for the s- and p-polarized lights.

At high voltages, the s-polarized light sees LC directors orthogonal to its polarization, whereas the p-polarized light sees periodically changing director orientations of LC. This periodic variation in director orientations gives rise to a corresponding periodic spatial modulation of the refractive index for the p-polarized light, whereas it produces no modulation effects for the s-polarized light. Therefore, the first-order diffracted intensity for the s-polarized light is expected to increase initially, reach a maximum at an intermediate voltage, and thereafter decrease at saturating voltages, as shown in Fig. 3b. It is interesting to note that the diffraction intensity is higher at saturating voltages than at 0 V. The reason is the weak diffraction effect, due to the presence of periodic electrodes, which is negligible at 0 V because it is screened by random light scattering but remains at saturating voltages. Similarly, for the s-polarized light, the monotonic increase in the zeroth-order diffraction intensity with increasing voltage can be easily explained by a decrease in random light scattering.

However, the results for the p-polarized light require an elaborate explanation. With increasing voltage, spatial modulation of the refractive index causes a corresponding phase shift modulation, as well as an amplitude modulation of the incoming p-polarized light; these combined modulation effects generate diffraction grating effects. Figure 4 illustrates the schematic phase-shift distributions at several different voltages. At low voltages, the intensity of the electric field is high enough to reorient the LC molecules only near the edges of the electrodes and therefore the phase shift, $\Delta\varphi$, reaches its maximum in these regions, as shown in Fig. 4a. At intermediate voltages, LC molecules in the inter-electrode regions become influenced by the electric field, resulting in a phase-shift distribution, as shown in Fig. 4b. At high

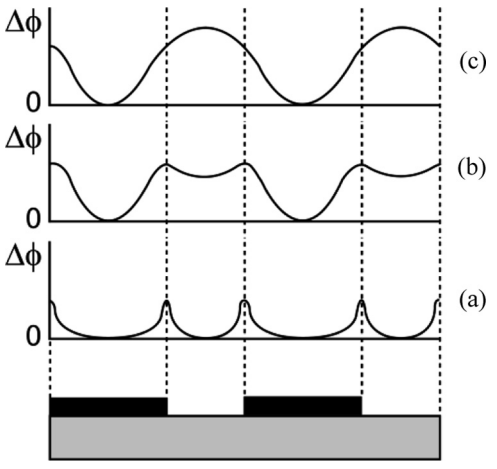

Figure 4. Schematic phase-shift distributions at (a) low voltages, (b) intermediate voltages, and (c) high voltages.

voltages, LC molecules align along the local electric field so that the phase shift reaches a maximum in the regions between electrodes, as shown in Fig. 4c. Note that LC molecules in the region close to the upper plate are less affected by the electric field, so the schematic phase-shift distributions in Figs. 4a–4c may be somewhat different from the actual distributions. Furthermore, a small amount of phase shift due to the presence of periodic electrodes is neglected.

As a result, the zeroth-order intensity gradually decreases with increasing voltage, whereas the first-order intensity gradually increases. This trend continues until the applied voltage reaches about 50 V. Above 50 V, the phase shift becomes too large, resulting in gradual disappearance of diffraction grating effects. Fucheda studied the diffraction for an ideal rectangular phase-shift distribution with two-step phase shifts of 0 and $\Delta\varphi$ and showed that the diffraction effects reached a maximum when $\Delta\varphi = \pi$ [8]. Though his simulated results are not strictly applicable to our IPS cells, our results can be explained qualitatively in a similar way. In our case, the phase difference of light, $\Delta\varphi$, in an electrode region and inter-electrode region first increases with increasing voltage and reaches π at about 50 V; thereafter, it continues increasing until it approaches 2π at saturating voltages. When $\Delta\varphi$ approaches 2π, the diffraction effect completely disappears, as shown in Fig. 3b.

When light passes through a PDLC cell consisting of LC droplets dispersed in a polymer matrix, the relative phase shift of light passing through a LC droplet to light traveling through the polymer matrix is given by

$$\Delta\varphi = \mathrm{k_p d}\left(\frac{n_d}{n_p} - 1\right), \tag{3}$$

where $\mathrm{k_p}$ is the wavenumber of light in the polymer matrix and d is the diameter of the LC droplets. $\mathrm{n_d}$ and $\mathrm{n_p}$ are the refractive indices of the LC droplet and the polymer matrix, respectively. It should be noted that $\mathrm{n_d}$ is electric field dependent and ranges from $\mathrm{n_o}$ to $\mathrm{n_e}$ of E7. When the applied voltage is high enough, $\mathrm{n_d}$ nearly equals $\mathrm{n_e}$ in the inter-electrode regions and $\mathrm{n_o}$ in the electrode regions. Therefore, the relative phase shift of light passing through these two regions can be approximated as

$$\Delta\varphi = \mathrm{k_o}\ \mathrm{d_{eff}}\ \Delta n, \tag{4}$$

where $\Delta\mathrm{n} = \mathrm{n_e} - \mathrm{n_o}$ and $\mathrm{k_o}$ is the wavenumber of light in free space. $\mathrm{d_{eff}}$ is the total distance that light travels passing through LC droplets. If we reasonably assume that $\mathrm{d_{eff}} \sim 3\mathrm{d}$, the phase shift is estimated to be $\Delta\varphi \sim 2\pi$ with $\Delta\mathrm{n} = +0.2246$, $\mathrm{k_o} = 2\pi/0\,6328\ \mu\mathrm{m}^{-1}$ and $d = 1\mu\mathrm{m}$ for the present work.

Cell 53A and Cell 75A

Similar measurements were performed for cell 53A, and the diffracted light intensities versus the applied voltage are plotted in Figs. 5a and 5b. Though the variations in intensity with the applied voltage are quite similar to those of cell 53B, a close comparison of Figs. 5a–5b with Figs. 3a and b reveals several distinctive characteristic features. First, the voltage at which the intensity of the zeroth diffraction order for the p-polarized light reaches a minimum decreases from 50 to 25 V, as seen in

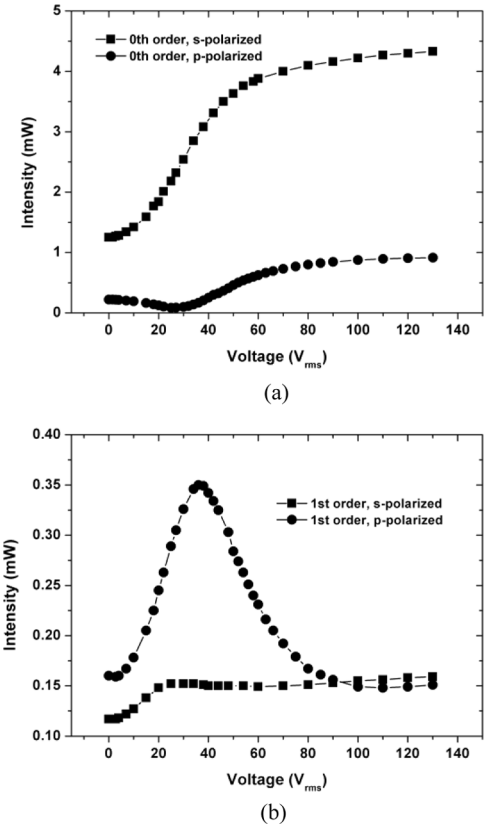

Figure 5. Diffracted intensities of cell 53A for the s- and p-polarized lights: (a) the zeroth diffraction order and (b) the first diffraction order.

Fig. 5a. Similarly, the peak voltages of the first diffraction order for the s- and p-polarized lights decrease from 50–55 to 25–36 V, as seen in Fig. 5b. Second, the diffracted intensities at 0 V have different values for the s- and p-polarized lights. Third, for the p-polarized light, the intensity of the first diffraction order for cell 53A is about a half that for cell 53B.

We can explain these observations by the influence of process A on cell 53A. When polymerization progresses under process A, strong UV irradiation not only permanently fixes the accumulation of the LC near the edges of electrode stripes but also secures the alignments of the LC directors to the local electric field. Because LC directors remain partially aligned, even after removal of the applied voltage, and more LCs are present near electrode edges where the electric field is very high, the diffracted light intensity should reach its minimum at lower voltages. It is obvious that different diffracted intensities in the absence of the applied voltage for the s- and p-polarized lights are the result of the partial alignment of LC directors in the direction orthogonal to the electrode stripes. An explanation for the decreased diffraction efficiency of the first diffraction order for cell 53A is less clear. It is possible that stripe-patterned LCs accumulated near the edges of electrodes destroyed periodicity of the phase shift and therefore deteriorated grating properties of the cell.

Additionally, we investigated cell 75A and present the experimental results, as shown in Figs. 6a, 6b, and 7. There are several notable features to discuss here. First, the peak voltage, V_p, of the first-order intensity for the p-polarized light decreases considerably down to about 18 V. Second, the intensity of the first diffraction order is high, even in the absence of an applied voltage. Moreover, at 0 V, the first-order diffraction intensities for s- and p-polarized lights are almost the same, whereas the zeroth- and second-order diffraction intensities are quite distinct. Third, the first- and second-order intensity curves for the p-polarized light, plotted as a function of the applied voltage, show local minima at 7 V. These observations can be explained as follows.

The shift of V_p to a lower voltage results from the persistence of the LC alignment and accumulation of LCs in edge regions of electrodes after removing the applied electric field. This behavior was previously discussed for cell 53A. High intensity of the first diffraction order at 0 V can also be accounted for by the remaining LC alignment. To understand the contradicting results of diffraction intensities at 0 V, we measured diffraction intensities as a function of the angle between polarization of light and electrode stripes, as shown in Fig. 7. In Fig. 7, angle $\theta = 0^\circ$ corresponds to the s-polarized light and 90° to the p-polarized light. The

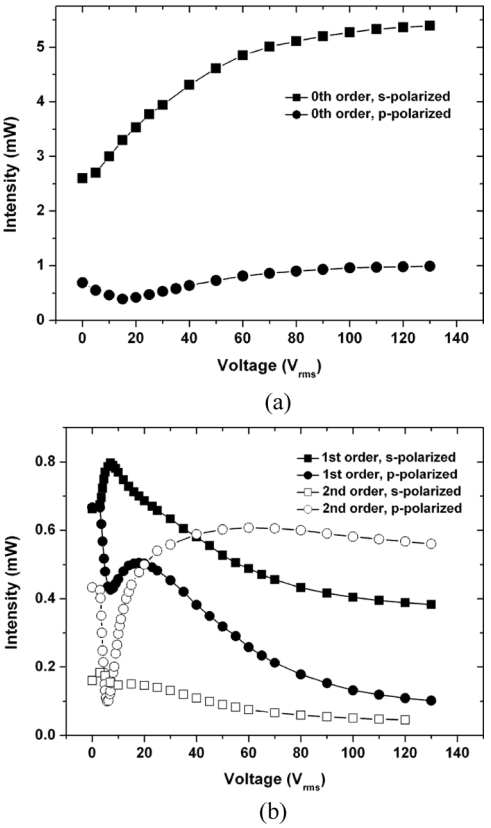

Figure 6. Diffracted intensities of cell 75A for the s- and p-polarized lights: (a) the zeroth diffraction order and (b) the first and second diffraction orders.

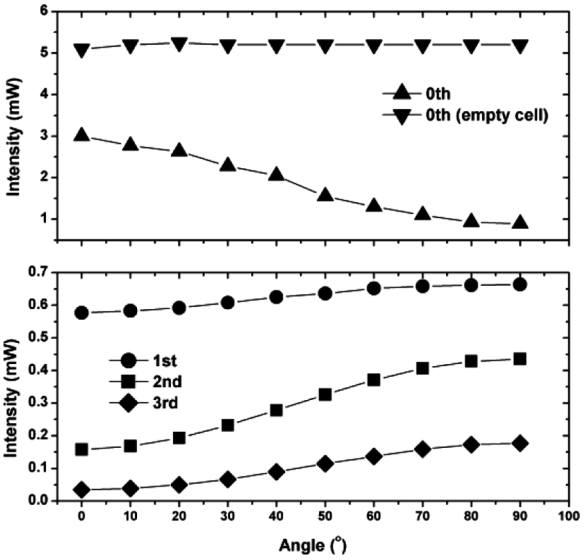

Figure 7. Diffracted intensities of cell 75A and an empty cell as a function of angle. Angle $\theta = 0^{\circ}$ corresponds to the s-polarized light and 90° to the p-polarized light.

zeroth-order intensity clearly demonstrates that LC directors are partially aligned at 0 V, and this result is consistent with Fig. 6a. The zeroth-order intensity for the empty cell shows no angle dependence and demonstrates that these results were not affected by electrode stripes. In contrast, high-order diffraction intensities increase with increasing angles. For instance, intensity ratios of the p-polarized light ($\theta = 90^{\circ}$) to the s-polarized light ($\theta = 0^{\circ}$), I_p/I_s, are 1.18, 2.75, and 5 for the first, second, and third orders, respectively. These results also support the partial alignment of LC directors at 0 V. It is interesting that diffracted intensities for the first and second orders are extremely sensitive to the voltage at low voltages, as shown in Fig. 6b. The optical microscope photograph of cell 75A shows that it has much more LC material accumulated in the form of a narrow, bright band near the electrode edges than cell 53A, as shown in Fig. 2c. Because the electric field is very high in this region, easy reorientation of LCs causes a corresponding change in the diffraction intensity. Therefore, the rapid initial decrease in the diffracted intensity and the existence of local minima at 7 V result from a transitory effect associated with a subtle change in director orientations at low voltages. This transitory effect gradually disappears with increasing voltage and the first-order intensity curve reaches a local maximum at about 18 V, generally showing the same behavior as the other two cells discussed.

Conclusions

In the present work, we fabricated two groups of grating cells based on PDLCs and studied their optical properties by measuring the diffraction intensities of the zeroth, first, and second diffraction orders as a function of the applied voltage and the angle. Our results show that diffraction intensities strongly depend on the applied voltage as well as the polarization of light. In particular, the intensity curve of the

first diffraction order for the p-polarized light has a bell-shaped peak, and the peak voltage, V_p, depends markedly on the preparation process and LC concentration. These results are promising for developing switchable diffraction gratings with controllable diffraction efficiency and optimum working voltage.

Acknowledgment

This research was supported in part by a Daegu University Research Grant (2008).

References

[1] Chen, J., Bos, P. J., Vithana, H., & Johnson, D. L. (1995). *Appl. Phys. Lett.*, *67*, 2588.
[2] Murai, M. (1993). *Liq. Cryst*, *15*, 627.
[3] Ramsey, R. R., & Sharma, S. C. (2005). *Optic. Lett.*, *30*, 592
[4] Crawford, G. P., & Bowley, C. C. (2000). *Appl. Phys. Lett.*, *76*, 2235.
[5] Fernandez-Nieves, A., Link, D. R., Rudhardt, D., & Weitz, D. A. (2004). *Phys. Rev. Lett.*, *92*, 105503.
[6] Resler, D. P., Hobbs, D. S., Sharp, R. C., Friedman, L. J., & Dorschner, T. A. (1996). *Opt. Lett.*, *21*, 689.
[7] Bouvier, M., & Scharf, T. (2000). *Optic. Eng.*, *38*, 2129.
[8] Fucheda, I. (2001). *Appl. Optic.*, *40*, 6252.
[9] Sakata, H., & Nishimura, M. (2000). *Jpn. J. Appl. Phys.*, *39*, 1516.
[10] He, W. T., Nose, T., & Sato, S. (1998). *Jpn. J. Appl. Phys.*, *37*, 4066.
[11] Abbate, G., Marino, A., & Vita, F. (2003). *Mol. Cryst. Liq. Cryst.*, *398*, 269.
[12] Lucchetta, D. E., Karapinar, R., Manni, A., & Simoni, F. (2002). *J. Appl. Phys.*, *91*, 6060.
[13] Jang, E., Kim, H.-R., Na, Y.-J., & Lee, S.-D. (2005). *Mol. Cryst. Liq. Cryst.*, *433*, 183.
[14] Rastegar, A., Skarabot, M., Blij, B., & Rasing, Th. (2001). *J. Appl. Phys.*, *89*, 960.
[15] Gibbons, W. M., Shannon, P. J., Sun, S.-T., & Swetlin, B. J. (1991). *Nature*, *351*, 49.
[16] Iimura, Y., Kusano, J., Kobayashi, A., Aoyagi, Y., & Sugano, T. (1993). *Jpn. J. Appl. Phys.*, *32*, L93.
[17] Jackson, J. D. (1999). *Classical Electrodynamics,* 3rd ed. John Wiley: New York.